Regular Article

ORGANIC CHEMISTRY RESEARCH
Published by the
Iranian Chemical Society
www.orgchemres.org

Org. Chem. Res., Vol. 5, No. 1, 51-63, March 2019.

3-(Propylcarbamoyl)acrylic Acid Functionalized Magnetic Nanoparticles Grafted to Poly (*N*-isopropylacrylamide-co-Acrylic Acid) Hydrogel: LCST and Drug Release

A.R. Karimi*, Z. Tajabadi, A. Khodadadi and F. Abdi

Department of Chemistry, Faculty of Science, Arak University, Arak 38156-8- 8349, Iran;
Department of Nanosciences & Nanotechnology, Arak University, Arak, Iran

(Received 1 June 2018, Accepted 14 August 2018)

In this research, to overcome the low mechanical properties of hydrogels based on poly *N*-isopropylacrylamide (PNIPAAm) and improve their stimuli responsive behavior and lower critical solution temperature, LCST, a new kind of hybrid magnetic nanoparticles was designed, prepared, and then grafted to (PNIPAAm-co-AAc) hydrogel through *in situ* dispersion copolymerization route. 3-(propylcarbamoyl)acrylic acid functionalized silica-coated magnetic nanoparticles (PC-AAc/MNPs) was prepared and used as a template for *in situ* dispersion copolymerization of the poly *N*-isopropylacrylamide (PNIPAAm) and acrylic acid (AAc) in the presence of methylene-bis-acrylamide as a cross-linking agent *via* free radical cross-linking polymerization. Also, controlled drug release behavior of metronidazole was investigated with prepared nanocomposite hydrogels. The vibrating sample magnetometer (VSM) illustrated superparamagnetic behavior for (PC-AAc/MNPs) and nanoparticles grafted hydrogel. Scanning electron microscopy (SEM) image of functionalized magnetic nanoparticles showed that they are spherical in shape and have the spherical structure with a diameter of about 15-30 nm. Moreover, the lower critical solution temperature (LCST) of the (PC-AAc/MNPs-g-PNIPAAm-co-AAc) hydrogel, as well as the onset temperatures, measured by the cloud point (CP) method at ~42 °C. Combined magnetic properties and thermosensitive behavior of (PNIPAAm-co-AAc) grafted magnetic nanoparticles could be utilized in controlled drug-targeting delivery. Hence, metronidazole as a model drug loaded on the magnetic hydrogel nanocomposite and the amount of drug release were measured by UV-Vis spectroscopy.

Keywords: Magnetic polymer, Hydrogels, Nanocomposites, Drug delivery systems, LCST

INTRODUCTION

The ability of smart polymers to response to several external stimuli including temperature, pH, light, magnetic fields and others make them as remarkable and interesting materials for various applications in diverse fields such as medicine [1], biomedicine [2], nanomedicine [2], biotechnology [3], artificial organs [4], optical data storage [5], sensors and smart textiles [6].

Among such smart polymers, hydrogels have interesting properties and are able to absorb large amounts of water, and have been widely used as most promising systems for biomedical and pharmaceutical applications especially delivery systems [7]. Hydrogels based on poly (*N*-isopropylacrylamide) (PNIPAAm) possess drug-loading ability in lots of *in vitro* applications [8-10] due to their stimuli-responsiveness properties. Although these hydrogels have very interesting properties and wide applications in drug delivery, they suffer from some drawbacks such as low mechanical strength and low LCST which limit their practical applications in biomedical fields [11-13].

A desirable phase transition temperature of these materials should be at or near the physiological temperature (37 °C). Therefore, improving the LCST and mechanical properties has become an important topic in the field of these hydrogel materials. Development of different strategies for improvement of performance and properties of hydrogels based on poly (*N*-isopropylacrylamide) has been

*Corresponding author. E-mail: a-karimi@araku.ac.ir

focus of many chemistry research activities over the years [14-16].

Applications of nanotechnology have been expanded in several branches of science and used in many fields, remarkably drug delivery investigations [17-18]. Therefore, the design and functionalization of new nanoparticles for preparation of new nanocomposite hydrogels in order to improve their properties for biomedical applications could be very valuable. Magnetic nanocomposite hydrogels have been recently emerged as versatile materials and studied in drug delivery carriers and tissue engineering, due to their distinctive properties such as stimuli responsive behavior, biological interactions, magnetic and optical properties, improved mechanical strength and remote actuation potential [19-21]. Incorporation of magnetic nanoparticles in the matrix of hydrogels in order to prepare magnetic nanocomposite hydrogels based on poly (*N*-isopropylacrylamide) could improve their stimuli responsive behavior, LCST and mechanical properties.

Due to our interest in the preparation of hydrogels and nanocomposite hydrogels [16,22-24], in current work, at first, superparamagnetic 3-(propylcarbamoyl)acrylic acid functionalized silica-coated magnetic nanoparticles (PC-AAc/MNPs) as a new kind of hybrid magnetic nanoparticles are prepared by reaction of 3-aminopropyl silica-coated magnetic nanoparticles (AP-MNPs) with maleic anhydride (MA) and grafted to (PNIPAAm-co-AAc) hydrogel through in situ dispersion copolymerization route. Finally, the properties, LCST behavior and metronidazole release of the nanocomposite hydrogel are investigated. Metronidazole (1-(2-hydroxyethyl)-2-methyl-5-nitro-imidazole) (MNZ), a nitroimidazole compound, is a gastric drug and has been used to treat diseases caused by bacteria and anaerobic protozoan infections. It has also been used as a promoter to induce the growth of cattle and pigs and improve feed efficiency [25]. The synthesized hydrogel nanocomposites as carriers allow delivery of the MNZ at the right time.

EXPERIMENTAL

Materials

Fe_3O_4 nanoparticles (MNPs) and Fe_3O_4@SiO_2 MNPs were prepared according to the literature procedure [26]. Ferric chloride hexahydrate ($FeCl_3.6H_2O$, 99%), ferrous chloride tetrahydrate ($FeCl_2.4H_2O$, 99%), tetraethyl orthosilicate (TEOS), dimethyl formamide (DMF, 99%), and acetone and ethanol (96%) were purchased from Merck. *N*-isopropylacrylamide (NIPAAm, 99%), *N,N'*-methylenebisacrylamide (BIS, $C_7H_{10}N_2O_2$, 99%), poly (*N*-vinylpyrrolidone) 25 (PVP, average Mw ~ 292.23 g mol^{-1}), (3-aminopropyl)trimethoxysilane (APTMS), maleic anhydride (MA) (99%) and dialysis bag for in vitro release studies were purchased from Sigma-Aldrich (St. Louis, USA). Acrylic acid (AAc, 99.5%) and potassium persulfate (KPS, $K_2O_8S_2$, 99%) were provided from Fluka (Sleeze, Germany). Metronidazole (Mw = 171.2 g mol^{-1}) was obtained from Kimiagaran Emrooz Chemical Ind. (Arak, Iran). Deionized water was used in all experiments.

Preparation of 3-(Propylcarbamoyl)acrylic Acid Functionalized Magnetic Nanoparticles (PC-AAc/MNPs)

Synthesis of 3-aminopropyl silica-coated magnetic nanoparticles (AP-MNPs). (Fe_3O_4@SiO_2 MNPs) (1 g) were dispersed in 40 ml toluene under ultrasonic irradiation for 1 h. After that, 1.4 ml (3-aminopropyl)trimethoxysilane (APTMS) was added into above dispersion. The mixture was stirred at 100 °C for 12 h under nitrogen atmosphere. The resultant product was obtained by magnetic separation and was thoroughly washed with ethanol and deionized water until neutral, then was dried at room temperature under vacuum for 1 day.

Preparation of (PC-AAc/MNPs) Magnetic Nanoparticles

A mixture of (AP-MNPs) (1 g) and maleic anhydride (MA) (1 g, 10.19 mmol) in DMF (20 ml) was irradiated with ultrasound at 60 °C for 30 min. Then, the mixture was stirred at 100 °C under nitrogen atmosphere for 6 h. Finally, the PC-AAc/MNPs solid was obtained by magnetic separation, and further washed with ethanol and deionized water, then was dried at 50 °C for 6 h under vacuum.

Preparation of PNIPAAm-co-AAc Hydrogel

NIPAAm (0.3 g), AAc (0.058 g, 0.8 mmol), BIS (0.0267 g, 0.173 mmol) as cross-linking agent and PVP (0.3 g) were mixed in 30 ml deionized water in a three-necked round bottomed flask (50 ml). The mixture was degassed by

purging with nitrogen for 40 min. Polymerization of the hydrogel was carried out at 70 °C for 6 h, using potassium persulfate (KPS, $K_2O_8S_2$) (0.013 g, 0.05 mmol) as redox initiator. After the polymerization, the synthesized hydrogel was immersed in distilled water at room temperature for 24 h and the water was refreshed every several hours in order to allow the unreacted chemicals to leach out. The final product was collected by centrifugation and dried under vacuum.

Synthesis of (PC-AAc/MNPs-g-PNIPAAm-co-AAc) nanocomposite hydrogel. Functionalized magnetic nanoparticles grafted to PNIPAAm-co-AAc hydrogel were prepared by in situ dispersion polymerization in water. In a typical procedure, NIPAAm (0.3 g, 2.5 mmol), AAc (0.058 g, 0.8 mmol), BIS (0.0267 g, 0.173 mmol) as cross-linking agent and PVP (0.3 g) as a steric stabilizer were dissolved in 30 ml deionized water in a three-necked round bottom flask equipped with a nitrogen gas inlet and a condenser. Then, PC-AAc/MNPs magnetic nanoparticles (5 wt%) were dispersed in 2 ml deionized water under ultrasonic irradiation and added to the reaction mixture. The solution was stirred and heated to 70 °C for 40 min under continuous purging with nitrogen atmosphere to exclude dissolved oxygen. Next, the initiator, KPS (0.013 g, 0.05 mmol), dissolved in 2 ml of deionized water was added to the mixture to start polymerization. The reaction was carried out at 70 °C for 6 h under N_2. After that, the synthesized hydrogel nanocomposites were immersed in distilled water at room temperature for 6 h and the water was refreshed every several hours in order to allow the unreacted chemicals to leach out. Unreacted nanoparticles were separated by a magnetic field, and the final PC-AAc/MNPs magnetic nanoparticles grafted to PNIPAAm-co-AAc hydrogel was collected by centrifugation at 4000 rpm and dried under vacuum.

LCST Measurement of (PNIPAAm-co-AAc) Hydrogel and (PC-AAc/MNPs-g-PNIPAAm-co-AAc) Nanocomposite Hydrogel

The thermal behavior or LCST of the (PNIPAAm-co-AAc) hydrogel and (PC-AAc/MNPs-g-PNIPAAm-co-AAc) nanocomposite hydrogel were determined by UV-Vis spectrophotometer coupled with a temperature controller. So, 0.025 g of (PNIPAAm-co-AAc) or (PC-AAc/MNPs-g-PNIPAAm-co-AAc) was swelled completely in 15 ml deionized water and the optical transmittance was determined at various temperatures (25-50 °C with 2 °C intervals).

Drug-loading of (PC-AAc/MNPs-g-PNIPAAm-co-AAc) Hydrogel

Metronidazole was used as model drug for controlled drug release demonstration. This compound was chosen as a model drug due to its high aqueous solubility. In brief, metronidazole loaded hydrogel nanocomposite was prepared by incubation of 0.1 g of dry PC-AAc/MNPs-g-PNIPAAm-co-AAc in drug solution (0.05 g/5 ml) for 1 day and was stirred well to load the metronidazole into the hydrogel. Then, the swollen nanocomposite loaded with drug was dried at 40 °C under vacuum for at least 48 h until there was no weight change.

In Vitro Drug Release from Magnetic Hydrogel Nanocomposite

To study drug release, metronidazole-loaded thermosensitive hydrogel nanocomposite was soaked in 6 ml phosphate buffer solution (PB) (pH = 7.4, 0.1 M) and then the swollen hydrogel was packed in a dialysis bag (MW cut-off 20000) and was incubated in 250 ml (PB) solution (pH = 7.4, 0.1 M) at 37 °C under mild agitation with shaking rate of 80 rpm. At specific time intervals, samples were withdrawn and replaced with 3 ml fresh buffer solution (the same volume of the released medium). The samples were filtered and analyzed using UV-Vis spectrometer. Moreover, the standard calibration curve of the absorbance as a function of drug concentration was studied using a UV spectrophotometer.

Characterization

Fourier transform infrared (FT-IR) spectra (Unicom Galaxy series, FT-IR 5000) of the samples were recorded in KBr pallets. X-ray diffraction spectroscopy (XRD) (X'Pert pro MPD, PANalytical with Cu Kα radiation) was used to investigate the crystal structure of the samples. Thermogravimetric analysis (TGA, Perkin-Elmer 6300 Pyris Diamond TM) was performed by heating from 30 °C to 1100 °C at a heating rate of 10 °C min^{-1} under nitrogen atmosphere. The morphologies and size of hybrid

nanoparticles were determined by scanning electron microscopy (SEM) (KYKY, EM3200). Magnetic properties were measured with a vibrating sample magnetometer (VSM, Lake Shore 7300) at room temperature. The LCST value was measured by the cloud point (CP) method with UV-Vis spectroscopy (Perkin-Elmer Lambda double beam) coupled with a temperature controller.

RESULTS AND DISCUSSION

Preparation and Characterization of 3-(Propylcarbamoyl)acrylic Acid Functionalized Magnetic Nanoparticles (PC-AAc/MNPs)

The functionalized magnetic nanoparticles were prepared according to the procedure shown in Scheme 1. Typically, PC-AAc/MNPs magnetic nanoparticles were prepared in four steps. The first time, Fe_3O_4 nanoparticles were prepared by a chemical co-precipitation of Fe^{2+} and Fe^{3+} ions under alkaline condition. Then, Fe_3O_4 nanoparticles were subsequently coated with silica (Fe_3O_4@SiO_2) through the well-known Stober method [27]. After that, the Fe_3O_4@SiO_2 structure was sequentially treated with (3-aminopropyl)trimethoxysilane (APTMS) that can bind covalently to the free-OH groups at the surface of the particles. Finally, reaction of the 3-aminopropyl-functionalized magnetic silica nanoparticles (AP-MNPs) with maleic anhydride gives 3-(propylcarbamoyl)acrylic acid functionalized magnetic nanoparticles (PC-AAc/MNPs) as a template site for a radical polymerization.

The as-prepared functionalized magnetic nanoparticles were also characterized by Fourier transform infrared spectroscopy (FTIR), X-ray diffraction (XRD), field emission scanning electron microscopy (FE-SEM), the energy dispersive X-ray (EDX), vibrating sample magnetometry (VSM), and thermogravimetric analysis (TGA). Figure 1 shows the FT-IR spectrum of Fe_3O_4, Fe_3O_4@SiO_2, AP-MNPs and PC-AAc/MNPs magnetic nanoparticles in the wavenumber range 4000-400 cm^{-1}. FT-IR spectrum of the bare magnetic Fe_3O_4 nanoparticles displayed the peak around 578 cm^{-1} attributed to the stretching vibration mode of Fe-O bonds in Fe_3O_4 (Fig. 1a). The peaks at 1099 cm^{-1} and 960 cm^{-1} in Fig. 1b are attributed to asymmetric stretching and symmetric stretching of the Si-O-Si group on Fe_3O_4@SiO_2 spectrum. In the FT-IR spectrum of AP-MNPs (Fig. 1c), the peak at 3447 cm^{-1} is related to NH_2 group. In this spectrum presence of the anchored alkyl groups is confirmed by the weak aliphatic C-H symmetric stretching vibrations at 2933 cm^{-1}. Figure 2d shows the FT-IR spectrum of PC-AAc/MNPs magnetic nanoparticles. The absorption peaks at 1710 cm^{-1} and 1653 cm^{-1} are assigned to the stretching vibration mode of C=O and the peak at 1599 cm^{-1} should be attached to the stretching vibrations of the C=C bond. All of these revealed the ring-opening reaction of the maleic anhydride. Finally, the FT-IR spectra of the functionalized magnetic nanoparticles indicated that the reactive groups had been introduced onto the surface of Fe_3O_4 nanoparticles.

The size and morphology of PC-AAc/MNPs magnetic nanoparticles were examined by scanning electron microscopy (SEM). Figure 2 shows the general morphology of the functionalized magnetic nanoparticles, clearly indicating that the particles have the spherical structure with a diameter of about 15-30 nm.

The energy dispersive X-ray spectroscopy (EDS) results, obtained from SEM analysis of PC-AAc/MNPs magnetic nanoparticles, shown in Fig. 3, clearly displays the presence of Si, C, O, N and Fe in the functionalized magnetic nanoparticles. In addition, EDS signals indicate that the Fe_3O_4 nanoparticles are loaded into silica, and the higher intensity of the Si peak compared with the Fe peaks shows that the Fe_3O_4 nanoparticles were trapped by SiO_2. According to the above analysis, This analysis confirms that the functionalized silica-coated magnetic nanoparticles have been successfully synthesized.

X-ray diffraction (XRD) patterns of the PC-AAc/MNPs magnetic nanoparticles is shown in Fig. 4a. The XRD data of the synthesized functionalized magnetic nanoparticles show diffraction peaks at 2θ = 30.24°,35.03°, 43.24°, 53.66°, 57.11°, 62.73° and 74.25° that can be assigned to the seven indexed planes (220), (311), (400), (422), (511), (440) and (533), respectively, indicating that the Fe_3O_4 particles in the nanoparticles were pure Fe_3O_4 with a crystalline cubic spinel structure; these match well with the standard Fe_3O_4 sample (JCPDS card no. 85-1436). The broad peak from 2θ ~ 15° to 27° is consistent with an amorphous silica phase in the shell of the silica-coated Fe_3O_4 nanoparticles (Fe_3O_4@SiO_2). The results indicated that functionalization does not change the crystalline phase

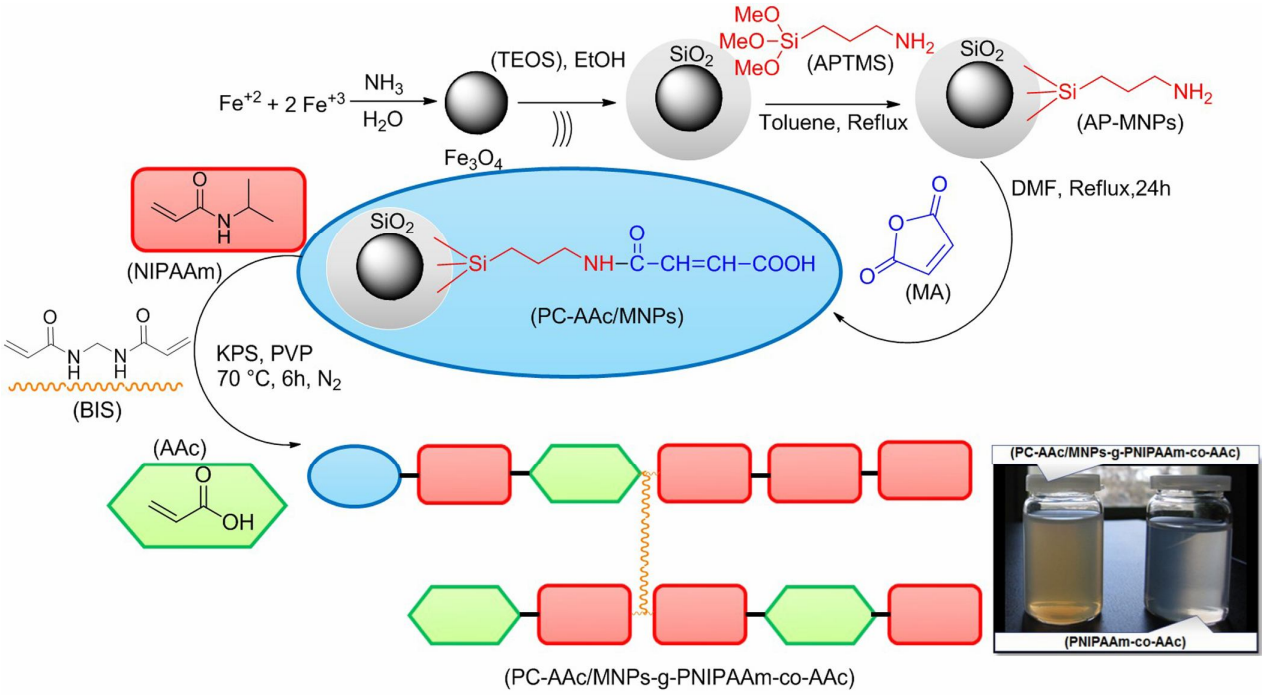

Scheme 1. Preparation of (PC-AAc/MNPs) nanoparticles and (PC-AAc/MNPs-g-PNIPAAm-co-AAc) hydrogel

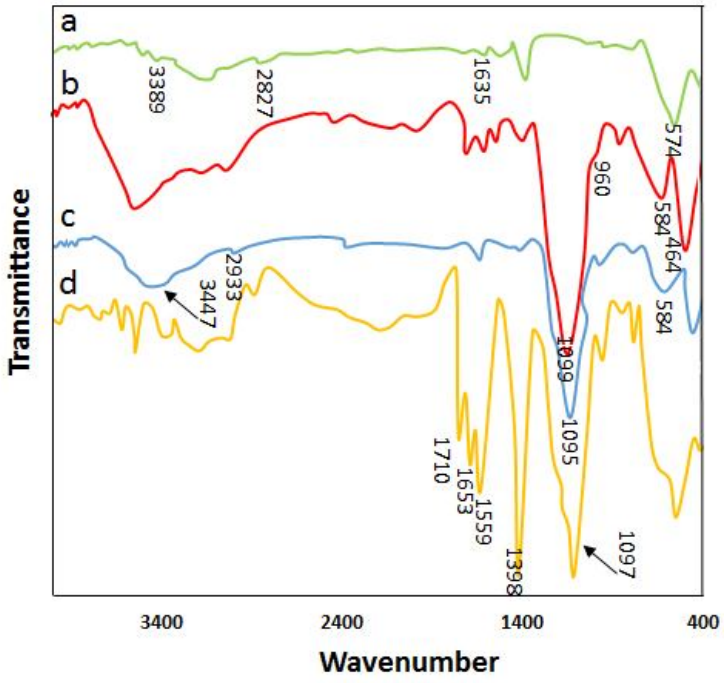

Fig. 1. The comparative FT-IR spectra for (a) Fe_3O_4, (b) Fe_3O_4@SiO_2, (c) AP-MNPs and (d) PC-AAc/MNPs.

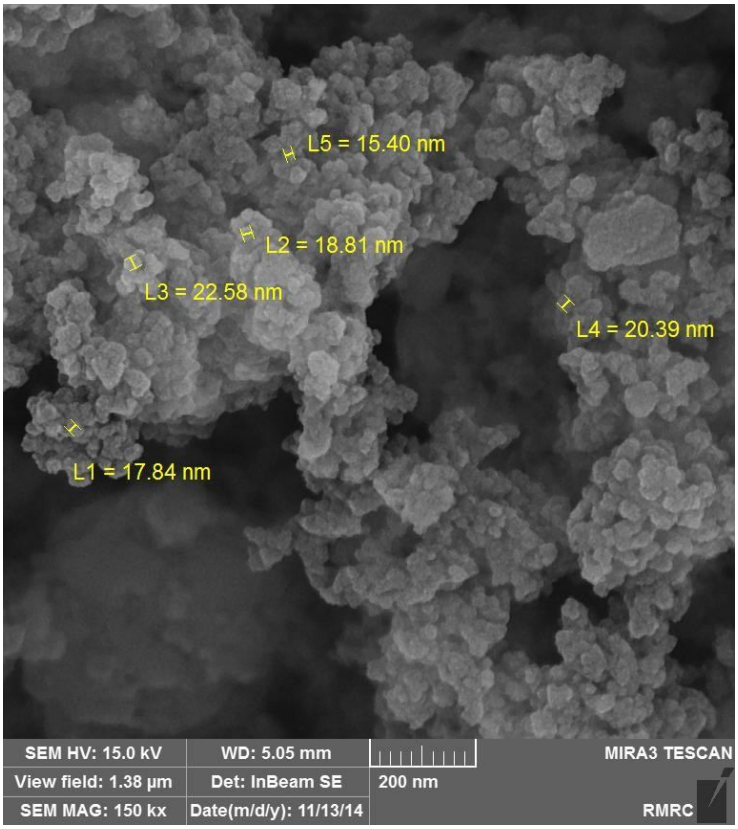

Fig. 2. FE-SEM images of PC-AAc/MNPs magnetic nanoparticles.

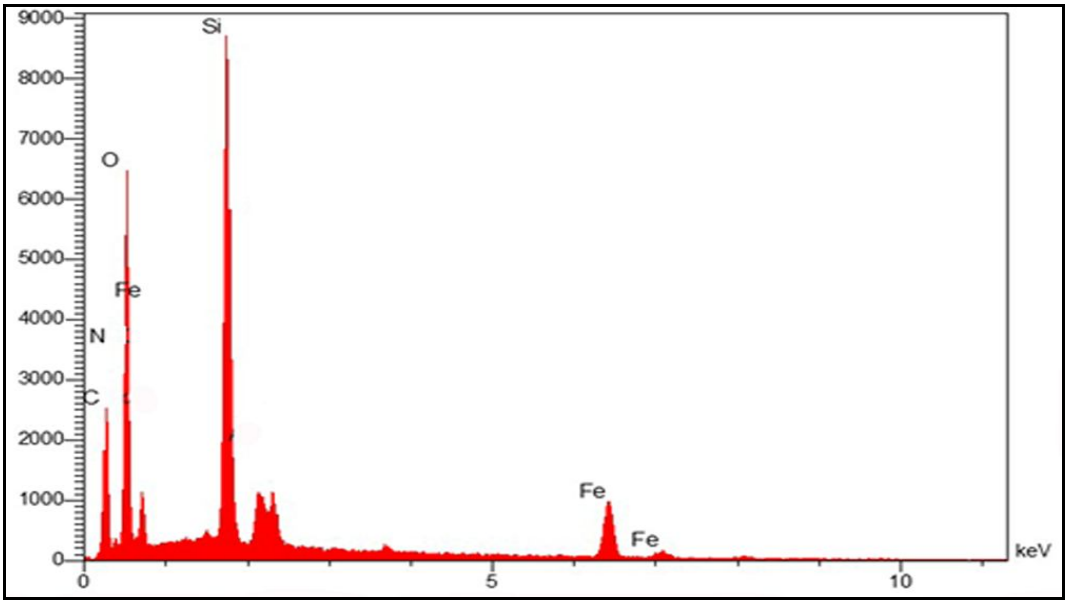

Fig. 3. EDS spectrum of PC-AAc/MNPs magnetic nanoparticles.

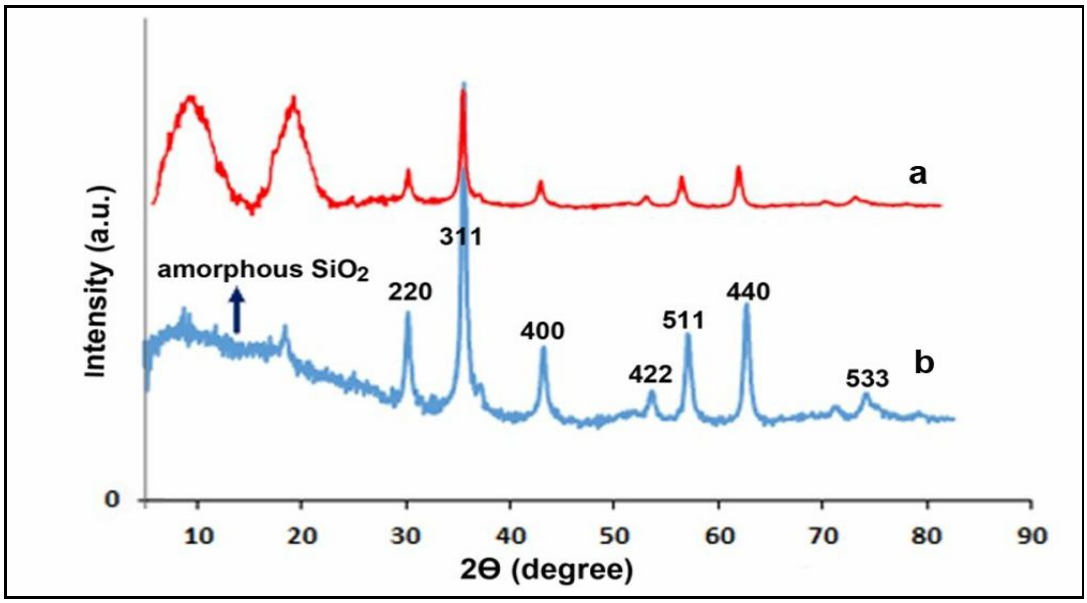

Fig. 4. X-ray diffraction (XRD) pattern of (a) PC-AAc/MNPs magnetic nanoparticles, and (b) (PNIPAAm-co-AAc) grafted to PC-AAc/MNPs magnetic nanoparticles.

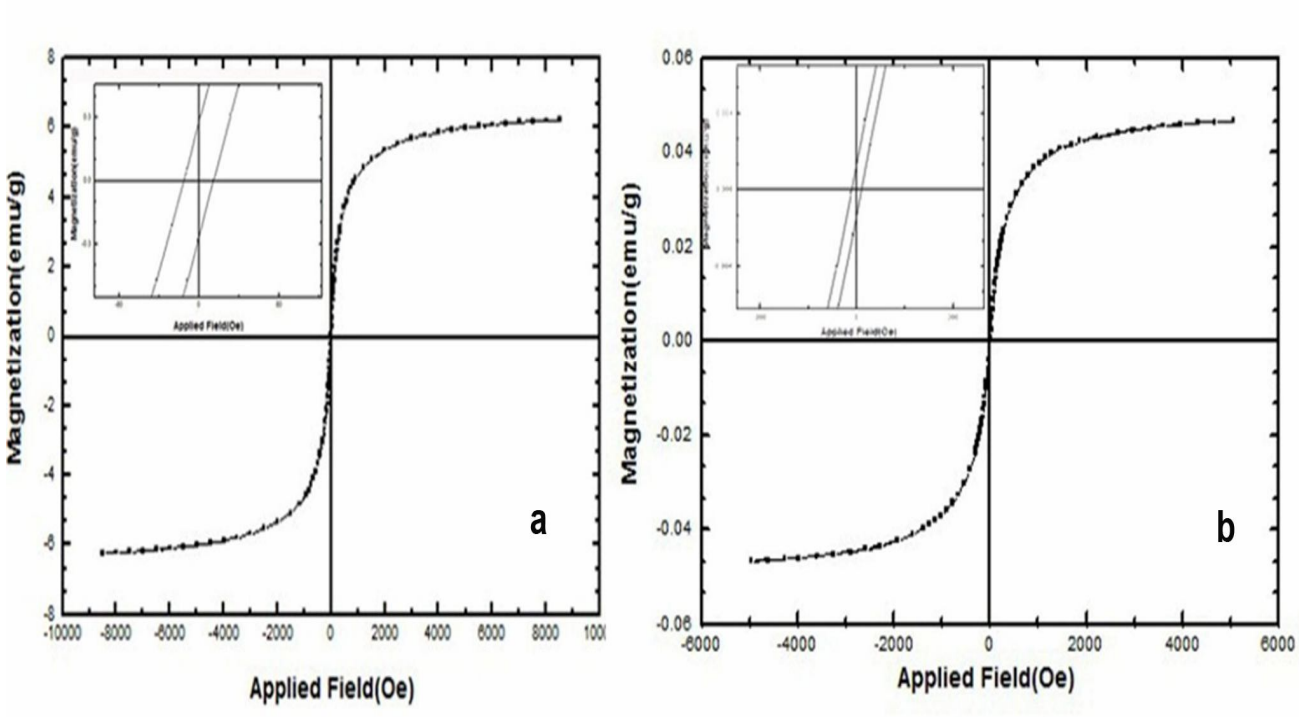

Fig. 5. Magnetization curve of (a) PC-AAc/MNPs magnetic nanoparticles, and (b) magnetization curve of the (PNIPAAm-co-AAc) grafted to PC-AAc/MNPs magnetic nanoparticles.

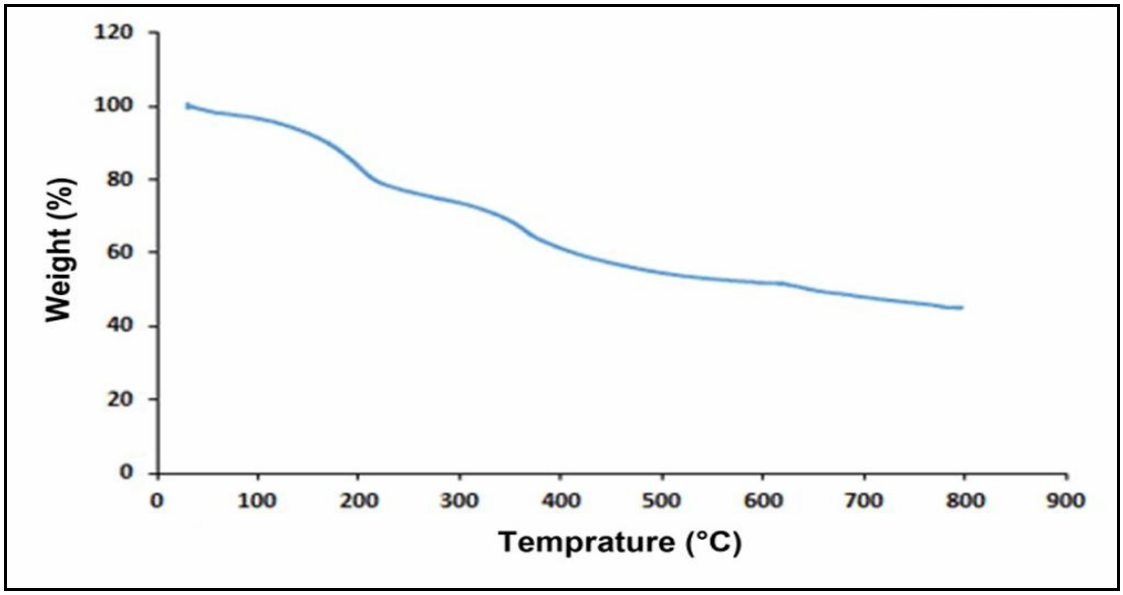

Fig. 6. The TGA thermogram of the PC-AAc/MNPs magnetic nanoparticles.

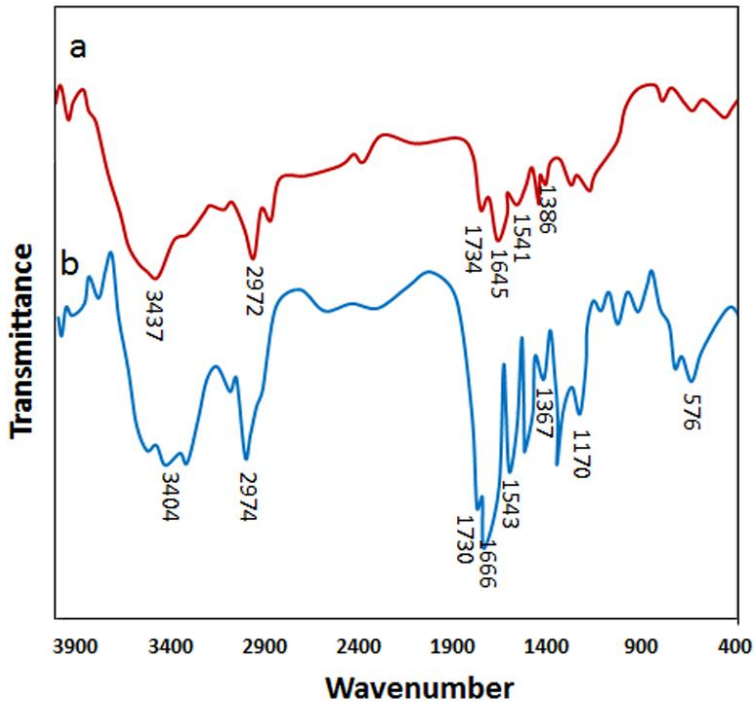

Fig. 7. The comparative FT-IR spectra for (a) PNIPAAm-co-AAc hydrogel, and (b) PC-AAc/MNPs magnetic nanoparticles grafted to PNIPAAm-co-AAc hydrogel.

of Fe_3O_4. The average crystalline diameter (D) was found to be 36.18 nm, taken/extracted from the scherrer's equation $D = K\lambda/(\beta\cos\theta)$.

The magnetic behavior of PC-AAc/MNPs magnetic nanoparticles was measured by vibrating sample magnetometer (VSM) at room temperature (Fig. 5a). The magnetization curve of the magnetic nanoparticles shows the superparamagnetic behavior with saturation magnetization (M_s), coercivity (H_c) and remanent magnetization (M_r). The magnetization of samples could be completely saturated at high fields of up to ±8000.0 Oe. In addition, the hysteresis loops exhibit the superparamagnetic behavior of the nanoparticles in which M_r and H_c are close to zero (M_r = 6.2 emu g^{-1} and H_c = 0.27 Oe, respectively). The superparamagnetic behavior prevents nanoparticles aggregation and makes them disperse when the external magnetic field is removed. So, this is the most important property in drug release [28].

The TGA thermogram of the PC-AAc/MNPs magnetic nanoparticles is shown in Fig. 6. The results showed two weight loss steps around 120-800 °C. The first weight loss below 120 °C is related to removal of trapped solvent such as water. The second weight loss step at about 120 °C to nearly 800 °C is attributed to the decomposition of the coating organic layer in the functionalized magnetic nanoparticles. So, the weight loss around 120-800 °C gives the organic grafting ratios of the magnetic nanoparticles that is about 52%.

Characterization of the Prepared PC-AAc/MNPs Magnetic Nanoparticles Grafted to PNIPAAm-co-AAc Hydrogel

To confirm the proposed structure of hydrogel nanocomposite, FT-IR spectra of PNIPAAm-co-AAc hydrogel and PC-AAc/MNPs magnetic nanoparticles grafted to PNIPAAm-co-AAc hydrogel are shown in Fig. 7. In these spectra, the peaks at 1645, 1386 and 2972 cm^{-1} were attributed to amide (C=O stretching), isopropyl groups ($-CH(CH_3)_2$) and CH_3 asymmetric stretching band, respectively. The band at 1543 cm^{-1} were ascribed to the amide (-NH) functional group. The characteristic peak at 1734 cm^{-1} represents the C=O stretching vibration in the carboxyl groups of AAc units. The broad peaks at 3400-3450 cm^{-1} was assigned to water of hydration attached to the hydrogel polymer and COOH group [29]. In addition, comparing with the IR spectrum of PNIPAAm-co-AAc hydrogel (Fig. 7a), the IR spectrum of PC-AAc/MNPs magnetic nanoparticles grafted to PNIPAAm-co-AAc hydrogel (Fig. 7b) has additional absorption peak at 576 cm^{-1} attributed to stretching vibration of Fe-O in Fe_3O_4. It indicated that the reactive groups for polymerization have been introduced onto the surface of magnetite nanoparticles. Moreover, there are no peaks of C=C in this spectrum. As a result, the FT-IR spectrum of hydrogel nanocomposite provided supportive evidence that the $-CH=CH_2$ group has initiated polymerization of PNIPAAm and AAc polymer chains have been successfully grafted onto the functionalized Fe_3O_4 nanoparticles [30]. The PNIPAAm-co-AAc hydrogel and PC-AAc/MNPs magnetic nanoparticles grafted to PNIPAAm-co-AAc hydrogel are shown in Figure 7b.

The FESEM images of magnetic hydrogel nanocomposites after graft polymerization are shown in Fig. 8. The results show that the size of particles is changed to be 50-90 nm. It indicated that the surface functionalization has a significant influence on their dispersion and in vitro behavior that can be explained by the electrostatic repulsion force and steric hindrance between the polymer chains on the surface of Fe_3O_4 nanoparticles.

Figure 4b shows the XRD pattern of magnetic hydrogel nanocomposite. The diffraction pattern of PNIPAAm-co-AAc grafted to functionalized Fe_3O_4 nanoparticles exhibited strong broad peaks at about $2\theta \sim 5°$ and 20° that corresponded to the amorphous structures of the hydrogel. The small diffraction peaks at around 2θ = 30.24°, 35.03°, 43.24°, 53.66°, 57.11°, 62.73° and 74.25° are attributed to the peak normally observed for the crystal structure of Fe_3O_4 nanoparticles, however, the peaks intensity decreased due to low content of nanoparticles. The results indicated that Fe_3O_4 retains its crystal structure in the hydrogel.

The magnetic properties of the hydrogel nanocomposite at room temperature are shown in Fig. 5b. The saturation magnetization (Ms) of the (PNIPAAm-co-AAc) grafted to functionalized Fe_3O_4 was found to be 0.04 emu g^{-1}, less than that of the functionalized Fe_3O_4 nanoparticles (6.2 emu/g) and the Mr and the H_c were close to zero (M_r = 0.0013 emu g^{-1}, and H_c = 10.5, respectively). This difference suggests a large amount of polymers grafted on the surface

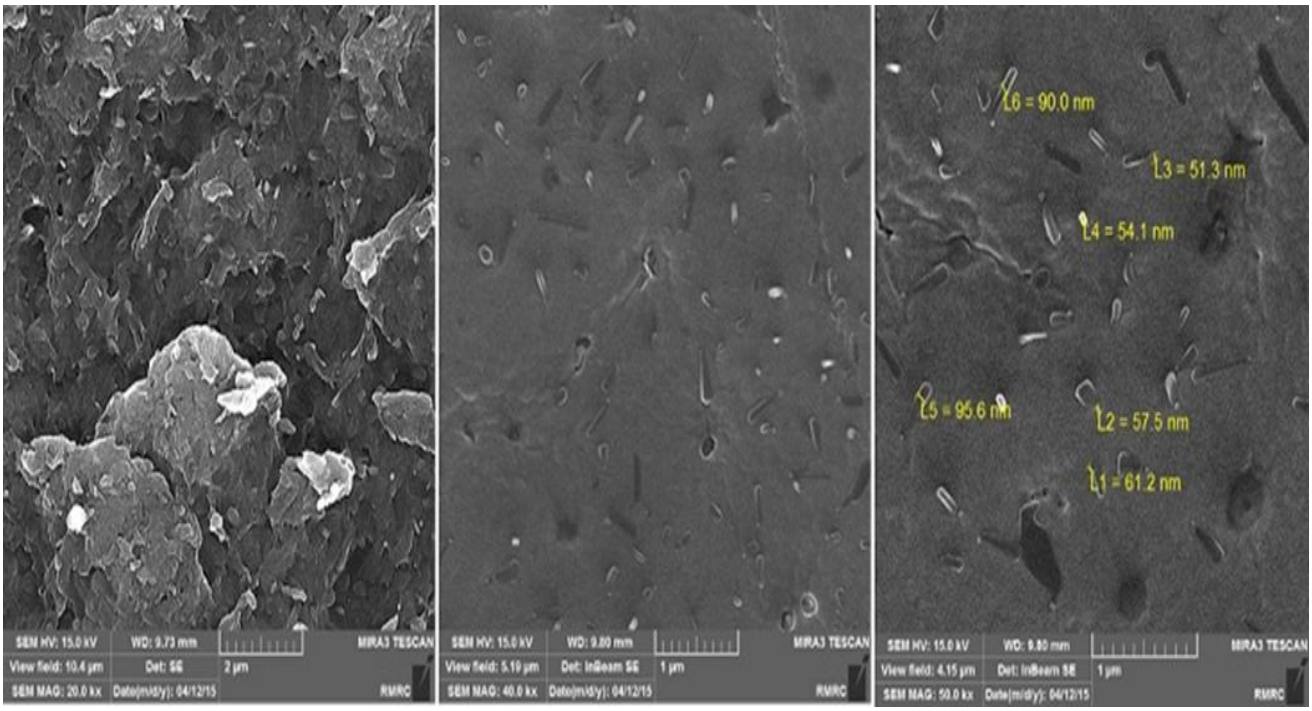

Fig. 8. The FESEM images of (PC-AAc/MNPs-g-PNIPAAm-co-AAc) hydrogel.

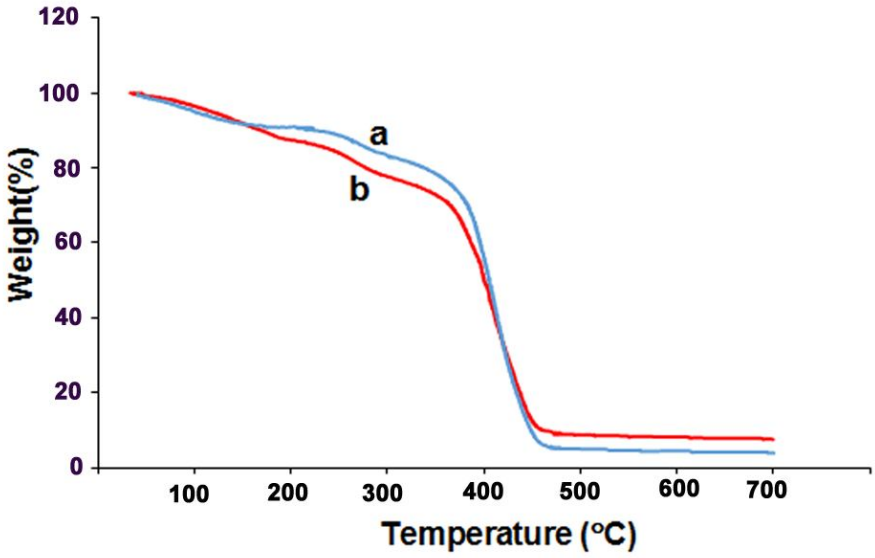

Fig. 9. The TGA thermogram of (a) (PNIPAAm-co-AAc) hydrogel, and (b) (PC-AAc/MNPs-g-PNIPAAm-co-AAc) Hydrogel.

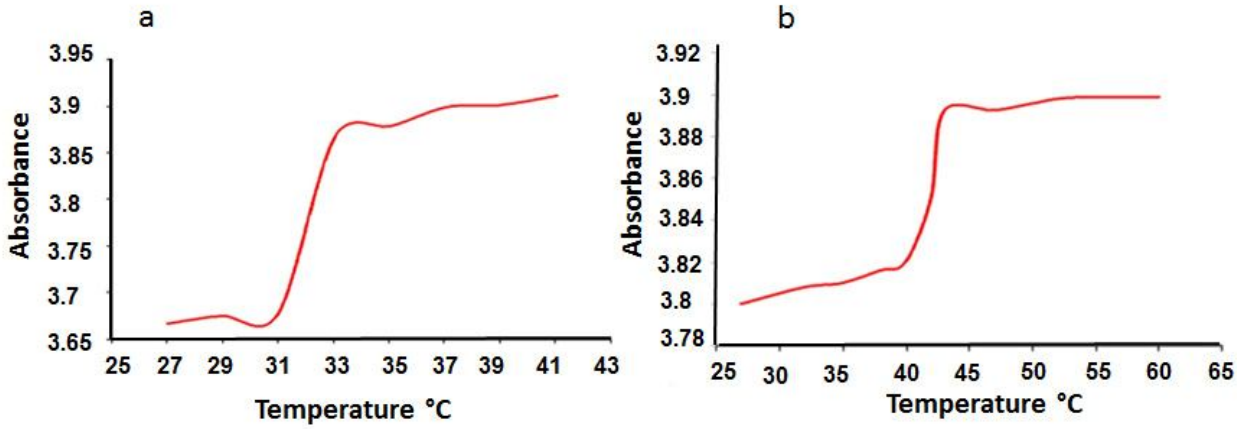

Fig. 10. The LCST of (a) (PNIPAAm-co-AAc), and (b) (PC-AAc/MNPs-g-PNIPAAm-co-AAc) hydrogel as measured by the cloud point method at pH 7.4.

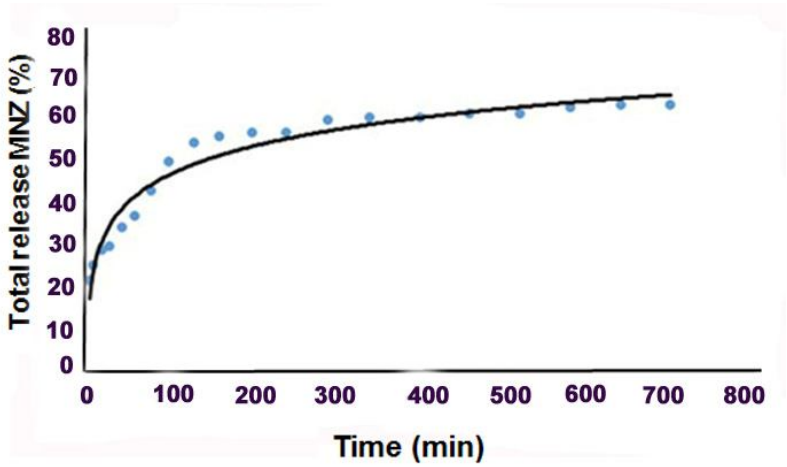

Fig. 11. Release curve of MNZ from the (PC-AAc/MNPs-g-PNIPAAm-co-AAc) hydrogel at pH 7.4 and 37 °C.

of Fe_3O_4 nanoparticles [31]. Moreover, the results showed that the functionalized Fe_3O_4 magnetic nanoparticles grafted to (PNIPAAm-co-AAc) hydrogel retained their superparamagnetic property in hydrogel matrix. These magnetic properties were critical in applications of the biomedical and bioengineering fields.

The effect of functionalized Fe_3O_4 magnetic nanoparticles grafted to (PNIPAAm-co-AAc) hydrogel on stability of the magnetic hydrogel nanocomposite was determined by the TGA analysis. The results are shown in Fig. 9. The (PNIPAAm-co-AAc) hydrogel (Fig. 9a) and the magnetic hydrogel nanocomposite (Figure 9b) began to decompose at around 120 °C. Moreover, the rate of weight loss between 120 and 380 °C is relatively slow representing the good thermal stability of them, and the maximum rate of lost weight for (PNIPAAm-co-AAc) and (PC-AAc/MNPs-g-PNIPAAm-co-AAc) was started from 380 °C. When the temperature is increased to 500 °C, the TGA curves of (PNIPAAm-co-AAc) hydrogel and the magnetic nanoparticles grafted to (PNIPAAm-co-AAc) hydrogel show a great weight loss of about 86.8 and 78.3 wt%, respectively, due to the decomposition of polymer matrix.

These results indicated that the thermal stability of the hydrogel nanocomposite increases slightly with hydrogel-grafted magnetic nanoparticles.

The LCST of the hydrogel nanocomposite was determined by UV-Vis spectrophotometer. However, the LCST of (PNIPAAm-co-AAc) hydrogels is lower than that of the human body temperature (37 °C). Therefore, they cannot be useful for drug delivery in the human body. As shown in Fig. 10, the LCST of (PNIPAAm-co-AAc) was 32 °C. Also, the phase transition of functionalized Fe_3O_4 magnetic nanoparticles grafted to (PNIPAAm-co-AAc) hydrogel occurs sharply at 42 °C. So, in the current work, the LCST values rise with magnetic nanoparticles grafted to the (PNIPAAm-co-AAc) hydrogel. The LCST of about 42 °C resembled the human body temperature. Therefore, that can be useful in drug-controlled release. In addition to the LCST measurement, the phase transition of the nanoparticles can easily be seen when the solution goes from clear to cloudy at each specific LCST.

Moreover, the release behavior of the hydrogel nanocomposite was studied for ~700 min in PBS (0.1 M, pH 7.4) at 37 °C. The release of metronidazole from hydrogel nanocomposite is plotted as a cumulative release with time in Fig. 11.

It shows an initial burst release of about 40-45% of metronidazole up to 100 min, followed by a more gradual release phase for the following 11 h. The initial fast release might be the result of the rapid dissolution of the metronidazole located at the hydrogel nanocomposite. After the burst release period, the rate of release fell as the dominant release mechanism was changed to drug diffusion through the hydrogel. The release medium penetrates into the particles and dissolves the entrapped drug and, therefore, it could be proposed that the major factor determining the drug release from nanoparticles is its solubilization or dissolution rate in the release medium.

CONCLUSIONS

In summary, a new thermo-sensitive magnetic nanocomposite hydrogel was prepared by in situ copolymerization method and was used successfully for the MNZ release as a model drug. For this purpose, PNIPAAm and AAc were bonded onto the surface of PC-AAc/MNPs magnetic nanoparticles by initiated radical polymerization in the presence of steric stabilizer poly (N-vinylpyrrolidone) (PVP) and methylene-bis-acrylamide (BIS) as a cross-linking agent. The saturation magnetization was found to be 6.2 and 0.04 emu g^{-1} for PC-AAc/MNPs magnetic nanoparticles and PC-AAc/MNPs magnetic nanoparticles grafted to poly (PNIPAAm-co-AAc) hydrogel, respectively, less than the pure Fe_3O_4 nanoparticles by VSM. These results confirmed that a large amount of silane and then copolymer efficiently grafted on the surface of Fe_3O_4 nanoparticles. Furthermore, the SEM, XRD and TGA results indicated that the PC-AAc/MNPs magnetic nanoparticles were embedded in the Poly (PNIPAAm-co-AAc) hydrogel. In addition, the grafting (PNIPAAm-co-AAc) hydrogel with modified Fe_3O_4 nanoparticles caused enhancement in the LCST of the hydrogel nanocomposite at 42 °C. The high temperature sensitivity of the prepared hydrogel nanocomposite suggests that it could be useful in biotechnology and targeted drug delivery applications.

ACKNOWLEDGEMENTS

We gratefully acknowledge the financial support from the Research Council of Arak University (Proposal number: 94/4827).

REFERENCES AND NOTES

[1] H.P. James, R. John, A. Alex, K.R. Anoop, Acta Pharm. Sin. B 4 (2014) 120.

[2] L.G. Gómez-Mascaraque, R. Palao-Suay, B. Vázquez, L.G. Gómez-Mascaraque, R. Palao-Suay, B. Vázquez, Smart Polym. Appl. (2014) 359.

[3] M. Talelli, A. Duro-Castaño, G. Rodríguez-Escalona, M.J. Vicent M. Talelli, *et al*. Smart Polym. Appl. (2014) 327.

[4] I.N. Savina, I.Y. Galaev, S.V. Mikhalovsky, Smart Polym. Appl. (2014) 408.

[5] E. Blasco, M. Piñol, C. Berges, C. Sánchez-Somolinos, L. Oriol, Smart Polym. Appl. (2014) 510.

[6] C. Cochrane, A. Cayla, Multidisciplinary Know-How for Smart-Textiles Developers (2013) 129.

[7] N.N. Ferreira, L.M.B. Ferreira, V.M.O. Cardoso, F.I.

Boni, A.L.R. Souza, M.P.D. Gremião, Polym. J. 99 (2018) 117.

[8] X. Zhou, J. Wang, J. Nie, B. Du, X. Zhou, *et al.* Polym. J. 48 (2016) 431.

[9] K. Li, X. Chen, Z. Wang, L. Xu, W. Fu, L. Zhao, L. Chen, K. Li, *et al.* Polym. Composite 38 (2017) 708.

[10] M. Pruettiphap, G.L. Rempel, Q. Pan, S. Kiatkamjornwong, Iran. Polym. J. 26 (2017) 957.

[11] F. Xu, J. Li, S. Yuan, Z. Zhang, E. Kang, K. Neoh, Biomacromolecules 9 (2007) 331.

[12] G. Fundueanu, M. Constantin, P. Ascenzi, Biomaterials 29 (2008) 2767.

[13] M.A. Ward, T.K. Georgiou, Polymers 3 (2011) 1215.

[14] M. Fathi, A.A. Entezami, A. Ebrahimi, K.D. Safa, Macromol. Res. 21 (2013) 17.

[15] A. Bajpai, S.K. Shukla, S. Bhanu, S. Kankane, Prog. Polym. Sci. 33 (2008) 1088.

[16] A.R. Karimi, F. Azadikhah, L. Rahimi, S. Ghadimi, Colloid Surf. A 484 (2015) 304.

[17] P. Kesharwani, B. Gorain, S.Y. Low, S.A. Tan, E.C.S. Ling, Y.K. Lim, C.M. Chin, P.Y. Lee, C.M. Lee, C.H. Ooi, H. Choudhury, M. Pandey, Diabetes Res. Clin. Pr. 136 (2018) 52.

[18] M. Gupta, V. Sharma, N.S. Chauhan, Nanostruct. Oral Med. 467 (2017) 510.

[19] N. Zhang, J. Lock, A. Sallee, H. Liu, Acs. Appl. Mater. Int. 7 (2015) 20987.

[20] A.L. Daniel-da-Silva, R.S. Carvalho, T. Trindade, Recent Patents on Nanotechnol. 7 (2013) 153.

[21] A.K. Hauser, R.J. Wydra, N.A. Stocke, K.W. Anderson, J.Z. Hilt, J. Control Release 219 (2015) 76.

[22] A.R. Karimi, A. Khodadadi, ACS Appl. Mater. Int. 8 (2016) 27254.

[23] S. Belali, A.R. Karimi, M. Hadizadeh, Polymer 109 (2017) 93.

[24] A.R. Karimi, M. Tarighatjoo, G. Nikravesh, Int. J. Biol. Macromol. 105 (2018) 1088.

[25] D. Chen, J. Deng, J. Liang, J. Xie, C. Huang K. Hu, Anal. Methods 5 (2013) 722.

[26] A.L. Morel, S.I. Nikitenko, K. Gionnet, A. Wattiaux, J. Lai-Kee-Him, C. Labrugere, B. Chevalier, G. Deleris, C. Petibois, A. Brisson, M. Simonoff, ACS Nano 2 (2008) 847.

[27] W. Stöber, A. Fink, E. Bohn, Colloid Interf. J. Sci. 26 (1968) 62.

[28] A. Akbarzadeh, M. Samiei, S. Davaran, Nanoscale Res. Lett. 7 (2012) 1.

[29] S. Davaran, S. Alimirzalu, K. Nejati-Koshki, H.T. Nasrabadi, A. Akbarzadeh, A.A. Khandaghi, M. Abbasian, S. Alimohammadi, Asian Pacific J. Cancer Prev. 15 (2014) 49.

[30] A. Akbarzadeh, M. Samiei, S.W. Joo, M. Anzaby, Y. Hanifehpour, H.T. Nasrabadi, S. Davaran, J. Nanosci. Nanotechnol. 10 (2012) 46.

[31] K. Petcharoen, A. Sirivat, Mater. Sci. Eng. 177 (2012) 421.